Enhanced ferroelectric polarization and possible morphotrophic phase boundary in PZT-based alloys

David S. Parker, Andreas Herklotz, T. Z. Ward, Michael A. McGuire, and David J. Singh

Phys. Rev. B **93**, 174307 — Published 16 May 2016

DOI: 10.1103/PhysRevB.93.174307

Enhanced ferroelectric polarization and possible morphotrophic phase boundary in PZT-based alloys

David S. Parker, Andreas Herklotz, T.Z. Ward, and Michael A. McGuire
Oak Ridge National Laboratory, 1 Bethel Valley Rd., Oak Ridge, TN 37831

David J. Singh
Dept. of Physics and Astronomy, University of Missouri, Columbia, MO 65211-7010

We present a combined theoretical and experimental study of alloys of the high performance piezoelectric PZT ($PbZr_{0.5}Ti_{0.5}O_3$) with BZnT ($BiZn_{0.5}Ti_{0.5}O_3$) and BZnZr ($BiZn_{0.5}Zr_{0.5}O_3$), focussing on atomic displacements, ferroelectric polarization, and elastic stability. From theory we find that the 75 - 25 PZT - BZnT alloy has substantially larger cation displacements, and hence ferroelectric polarization than the PZT base material, on the tetragonal side of the phase diagram. We also find a possible morphotrophic phase boundary in this system by comparing displacement patterns and optimized c/a ratios. Elastic stability calculations find the structures to be essentially stable. Experiments indicate the feasibility of sample synthesis within this alloy system, although measurements do not find significant polarization, probably due to a large coercive field.[a]

I. INTRODUCTION

Piezoelectricity, or the coupling of an internal electric field to strain, is typically tied to the formation of a morphotrophic phase boundary, or MPB, in the phase diagram of a material system which exhibits ferroelectricity. The MPB is an abrupt change in crystalline symmetry of a given material system as the relative proportion of two constituents of the material system changes continuously. For example, the widely used prototypical piezoelectric material $PbZr_{1-x}Ti_xO_3$ (PZT),[1] exhibits an MPB in a transition from a rhombohedral phase on the Zr-rich side to a tetragonal phase on the Ti-rich side around the x=0.5 midpoint, along with a "bridging" monoclinic phase. PZT is a particularly useful material in part because of its good performance and reasonable cost and also because its MPB is near-vertical, leading to relatively weak temperature dependence of properties.

There have been a number of advances[2–4] in piezoelectric materials, including the development of high performance piezocrystals, but PZT remains the material of choice for many applications. Here we explore the possibility of modifying PZT using some concepts originally developed for lead free electroceramics. Specifically, we explore the possibility of introducing A-site cation disorder involving Bi and Pb in the low Bi content regime to improve the properties of PZT.

We used first principles calculations to study the following alloy system: $Pb_{0.75}Bi_{0.25}Zr_{0.875-x}Ti_xZn_{0.125}O_3$ with x=0.375 and 0.5. This can be abbreviated as $(PZT)_{0.75}$-$(BZnT)_{0.25}$ and $(PZT)_{0.75}$-$(BZnZr)_{0.25}$, where B stands for Bi. The rationale for this choice of system for study is as follows: Firstly, we seek to *enhance* the piezoelectric performance of PZT, and so we begin with a system comparatively near the MPB of PZT. Secondly, it is well known[5] that in PZT, unlike in most B-site driven perovskite-based materials, the divalent A-site atom Pb plays a key role in the ferroelectricity. Periodic table neighbor Bi has a significantly smaller ionic radius (for six-fold coordination[6], 117 pm for Bi^{3+} versus 133 pm for Pb^{2+}) and as a consequence of this increased vibrational "room" can be expected to show yet more off-centering when placed in a material with majority A-site component Pb. A key point is that A-site disorder favors off-centering over octahedral tilts in many perovskites and so from a crystal chemical point of view it is plausible that Bi may strongly off-center in a PZT matrix rather than simply enhancing local octahedral tilts[7]. Indeed, our first principles calculations confirm this enhanced ferroelectric activity of Bi. The Zn is added to the composition to maintain charge balance and hence insulating character, and because there is evidence[8,9] for its utility in ferroelectric materials, as compared to other possible counter-ions.

II. FIRST PRINCIPLES CALCULATIONS - PROCEDURE

In order to understand the ferroelectricity, and potential for piezoelectric performance, in these PZT-based systems, we perform first principles calculations using the linearized augmented plane-wave (LAPW) density functional theory code WIEN2K[10]. We use the local density approximation (LDA) rather than the more commonly used generalized gradient approximation (GGA) since the LDA has been shown[11] to provide a more accurate description of ferroelectric phenomena, when used with experimental lattice parameters. We enforce this constraint by choosing all volumes equal to the experimental volume of PZT.

The calculations were done using supercells. These were chosen to satisfy both the requirements of appropriate stoichiometry as well as of a non-polar space group. The non-polarity is of particular importance since it ensures that any ferroelectric polarization computed in the calculation is an in-

[a] This manuscript has been authored by UT-Battelle, LLC under Contract No. DE-AC05-00OR22725 with the U.S. Department of Energy. The United States Government retains and the publisher, by accepting the article for publication, acknowledges that the United States Government retains a non-exclusive, paid-up, irrevocable, world-wide license to publish or reproduce the published form of this manuscript, or allow others to do so, for United States Government purposes. The Department of Energy will provide public access to these results of federally sponsored research in accordance with the DOE Public Access Plan (http://energy.gov/downloads/doe-public-access-plan).

trinsic result of the material under study, and not of an artificial asymmetry in structure. It turns out that for the systems studied here the minimum size cell meeting these criteria is a 2x2x2 supercell of the basic 5-atom perovskite unit cell, or a 40 atom cell.

For the calculations of PZT we have used sphere radii (in Bohr) of 1.45 for O, 1.9 for Zr and Ti, and 2.1 for Pb. For these calculations we used a 4x4x4 k-point grid, comprising 32 k-points in the irreducible Brillouin zone (IBZ). For the two PZT-based alloys studied we used somewhat different radii, of 1.4 for O, 1.83 for Zr, Zn and Ti and 2.1 for Bi/Pb, with a smaller 2x2x2 k-point grid, comprising 4 k-points in the IBZ. The smaller sphere radii were chosen to allow for the possibility of increased motion of the atoms of the PZT-based alloys, relative to PZT, since to determine an optimum c/a ratio it is essential that the sphere radii be identical for all modeled c/a ratios. For all materials the calculations used an RK_{max} of 6.75, where R is the smallest radius (the O atom) and K_{max} the largest planewave expansion vector. The smaller k-point grid of the PZT-based alloys, relative to PZT itself, was chosen to speed convergence as the relaxations of the PZT-based cells were arduous and time-consuming.

With this 2x2x2 supercell we study the two compositions mentioned above along with PZT itself ($PbZr_{0.5}Ti_{0.5}O_3$). Note that in the first two compositions we have chosen the Zr/Ti ratio to span the 1:1 ratio near to which the MPB appears in PZT, anticipating the possible appearance of an MPB in this composition range. We depict this supercell in Figure 1, where the centrosymmetric nature of the unit cell is apparent. Note that we have chosen an essentially rocksalt ordering of the Zr/Ti cations to maintain this symmetry. While in PZT itself there is little evidence for such cation ordering[12] this rocksalt ordering is essential for maintaining the proper centrosymmetry in a supercell. As mentioned, we choose the volume of the supercell to be the experimental volume of PZT itself at the MPB since, as is well known, ferroelectric instabilities are highly sensitive to volume.

Our strategy for studying the PZT-based compositions is as follows. For each composition, we construct a number of cells by varying the c/a ratio in the supercell, keeping the volume fixed. We then displace all 40 atoms from their symmetric positions in random amounts and directions, and then relax *all* atomic positions, with *no* symmetry constraints other than the chosen lattice parameters and the assumed orthogonality of the lattice vectors. The cell with the minimum energy for each of the two PZT-based compositions corresponds to the cell that would be observed in an experiment. Note that all calculational parameters, such as LAPW sphere radii, numbers of k-points, and plane-wave cut-off wave vector, are kept identical for all calculations, to ensure an "apples-to-apples" comparison. We depict the materials we will study on a ternary composition plot in the bottom panel of Fig. 1.

Care was taken to reach ground states in each calculation. We found various metastable local minima and eliminated them by repeating calculations with different starting structures including structures obtained by uniformly straining relaxed cells with other values of c/a.

Once the true ground states were achieved, the ferroelectric polarizations were computed by means of the Berry phase method using the BerryPI code[14]. The following method was used for the computations: firstly, the Born effective charge (BEC) of each of the atomic species was computed via a computation of the Berry phase difference $\Delta\phi$ resulting from displacement of all atoms of the same element in the [111] direction by an amount η varying between 0.002 and 0.005 lattice constants. From this change in phase the Born effective charge Z_i^* was obtained, for each Cartesian direction i, by means of the relation $Z_i^* = \frac{1}{2\pi}\frac{\Delta\phi_i}{\eta_i}$. These BEC values were then multiplied by the average atomic displacement relative to the symmetric positions to generate a computed ferroelectric polarization.

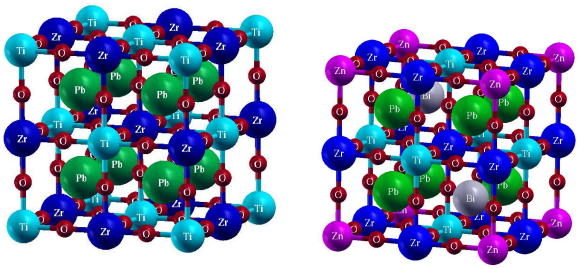

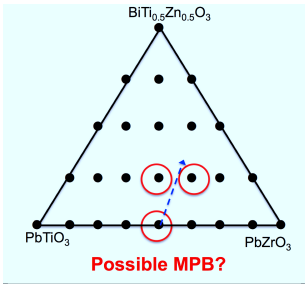

FIG. 1. The symmetric supercell showing (top left) PZT and (top right) the ordering of the Zr, Zn and Ti cations in PZT-BZnT. Zr atoms - dark blue, Zn - purple, Pb - green, Bi gray, Ti - light blue, O - red. Bottom: a ternary diagram showing the compositions studied in this work.

III. CALCULATED RESULTS - PZT

We begin by studying PZT itself. We displace all atoms randomly, optimize all internal coordinates and study the atomic displacement patterns of the atoms thus found, and resulting ferroelectric polarization, as a function of c/a ratio.

Presented in Figure 2 are the calculated energies of several strained structures of PZT ranging in c/a ratio from 0.90 to 1.10. The plot depicts a double-minimum structure, with energy increasing rapidly outside the two minima located at approximate c/a ratios of 0.98 and 1.06, and less rapidly between these two minima. The two minima are essentially degenerate in energy, with the calculated energies of the lowest two points (c/a=0.98 and 1.06) varying by less than 10 meV, or less than 0.25 meV per atom. This is in keeping with pre-

vious calculated results[5], which find the optimized tetragonal and rhombohedral structures to be degenerate within calculational accuracy. We note that we used here a fully ordered B-site lattice, which is an approximation that is needed in order to consistently treat this composition with the Bi containing cells below.

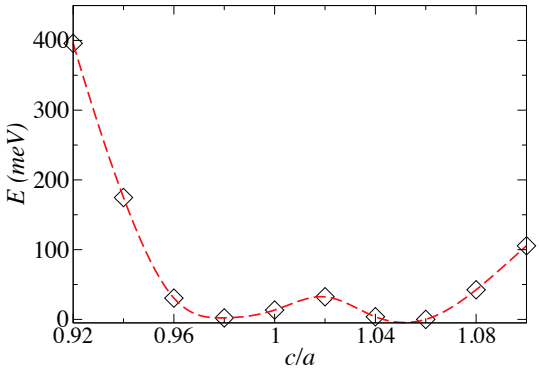

FIG. 2. (color online) The calculated energies of several optimized structures for the PZT compositions described in the text. Energy zero is set to the lowest calculated energy point.

We note that the c/a value of 1.06 found for PZT, while consistent with previous calculations is significantly greater than the actual c/a ratio for tetragonal PZT of approximately 1.022[13]. However, this discrepancy is not crucial, since the purpose of this work is to compare the potential ferroelectric properties of PZT-based materials with PZT itself. The calculated PZT c/a ratio of 1.06 can therefore be taken as a reference point for the tetragonality of the PZT-based alloys; indeed, we will observe a significant increase in tetragonality of the PZT-BZnT alloys, both theoretically and experimentally, relative to PZT.

It is of interest to look at the optimized structures of PZT in some detail. In Figure 3 we present the atomic displacements for the Pb, Zr, Ti and O atoms for the structures at the two degenerate energy minima - c/a=1.06 (left) and 0.98 (right). We begin with the left plot. It depicts average displacements, in Bohr, almost exclusively along the 001 axis, indicative of the tetragonality of PZT at this point. The displacements are largest for the Pb atom, in keeping with the generally A-site driven nature of ferroelectricity in this compound.

The displacement patterns, however, change radically for the c/a=0.98 structure (right of Figure 3). Unlike for c/a=1.06, here all the cations display substantial displacements in all three directions. The displacement patterns are largest for the x and y directions and smaller in the z-direction. As in the previous plot the Pb atoms show the largest displacements. Naively one might expect all displacements to be along the 111 direction, in light of the rhombohedral nature of PZT on one side of the MPB, but one recalls the existence of a monoclinic "bridging" phase in this system near the MPB. The c/a=0.98 displacement patterns may therefore depict the

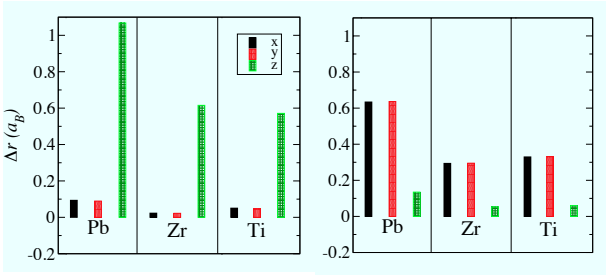

FIG. 3. (color online) The atomic displacements, relative to the center of the oxygen octahedral cages, of the optimized structures of PZT, with c/a ratios of 1.06 (left) and 0.98 (right). Note the great difference in the displacement patterns.

result of a competition between the monoclinic and rhombohedral phases.

The main point of these two plots is that they suggest the existence of the MPB in this system in a way that can be used for supercells with more complex compositions. We observe and discuss below a similar behavior in the PZT-derived compositions studied.

IV. CALCULATED RESULTS - PZT-BASED ALLOYS

Depicted in Figure 4 is the main result of our paper. We show the energies of the PZT-BZnZr (bottom) and PZT-BZnT (top) compositions as a function of c/a ratio. The plots display a great divergence in behavior, despite the substitution of just one atom out of the 40 in the supercell. This is suggestive, of a possible MPB in the vicinity of these compositions. In the top plot, the PZT-BZnT structure shows a minimum energy for a c/a ratio of approximately 1.08, which likely places it in the tetragonal regime. There is a secondary minimum at an approximate c/a ratio of 0.97, but this lies some 30 meV above this absolute minimum and is separated from it by a "hump" over 100 meV in height.

The situation is very different for the PZT-BZnZr plot in the bottom half of Figure 4. This has an absolute minimum for a c/a ratio of 0.97, a substantial distance from the 1.08 value for the other composition. There is a second subsidiary minimum at a c/a of unity, approximately 40 meV higher in energy. We have investigated carefully this region of parameter space to confirm that the states found are not metastable ones; the displacement patterns of these minima and near-minima points are quite similar which suggests that these are in fact the actual optimized structures.

A. Assessment of potential MPB in PZT- based alloys

To more directly assess the potential for an MPB in the vicinity of these two phases, in Figure 5 we present the observed displacement patterns for these two optimized structures (top left, PZT-BZnT, bottom left PZT-BZrT) as well as the metastable minima for these structures. In the top left plot

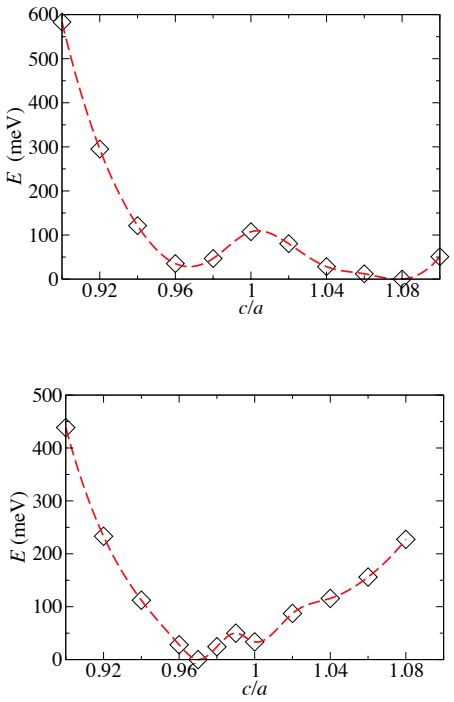

FIG. 4. (color online) The calculated energies of several optimized structures for the two PZT-based compositions described in the text. Top, PZT-BZnT; bottom; PZT-BZnZr. The symbols represent the calculated energies and the dashed line is a spline fit to these energies. Energy zero is set to the lowest calculated energy point.

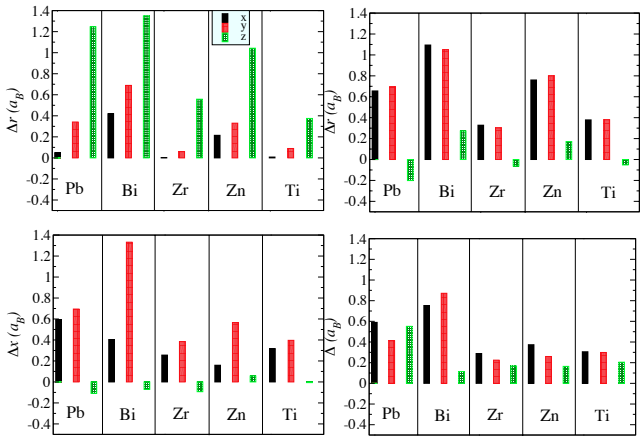

FIG. 5. (color online) The displacement patterns, relative to the center of the Oxygen octahedra, of the optimized (left) and metastable (right) minima structures for the two compositions described in the text. Top: PZT-BZnT; bottom PZT-BZrT.

(the PZT-BZnT composition) we observe the largest displacements to be z-axis displacements, as in the PZT plot for c/a= 1.06, though there are contributions from x and y as well. As expected the A-site displacements are predominant, with z-axis displacements exceeding 1 Bohr for both Pb and Bi. Note that the Bi displacements are larger than the Pb for all three axes, in keeping with its smaller ionic radius. Interestingly, the Zn displacement is also large, approaching 0.8 Bohr along the z-axis, which is surprising in view of its larger ionic radius than Zr and Ti. Although overall the atomic displacements are not entirely along the z-axis, these are the predominant ones and so this composition may be described as tetragonal.

The PZT-BZnZr composition (bottom left) shows very different behavior. Despite the substitution of just one Zr for one Ti, in a 40-atom supercell, the displacement patterns have changed *completely*. Here planar displacements predominate, with the Bi y displacement exceeding 1.4 Bohr. For all atoms the x and y displacement magnitudes substantially exceed the z-axis values - in some cases exceeding a ratio of 10:1. The planar displacement patterns here are fairly similar to those found above for PZT, although in that case the z-axis magnitudes were larger. Here the largest displacements are along the y-axis, though comparable displacements are found along the x-axis. Taken together these displacement patterns are suggestive of a monoclinic phase.

This possible monoclinic phase in the PZT-BZnZr phase would be of a very different character than the tetragonal phase found for PZT-BZnT and hints at an MPB in this composition range.

It is of interest to compare the ground state atomic displacement patterns for each composition with those of the metastable minima. For PZT-BZnT the metastable configuration, with c/a=0.96 (top right, Fig. 5) is very different from the ground state on the left, with planar displacements predominant in the former. The Bi displacements are as large as 1.1 a_B, comparable to those found for Bi (y-axis) in the ground state for PZT-BZrT. The Pb displacements are similarly comparable to those in PZT-BZrT, and somewhat surprisingly the Zn is large as well.

The differences from ground state to metastable minimum are smaller in the PZT-BZrT composition (bottom of Figure 5), and in fact here the metastable structure appears more nearly rhombohedral than the actual ground state. The smaller structural differences can be directly traced to the much closer c/a ratios of these two structures (the metastable structure has c/a =1.00, the ground state has c/a=0.97), compared to the 0.97 and 1.08 c/a values for the metastable and ground state structures for PZT-BZnT.

To make the preceding discussion more rigorous we consider the following. As defined previously, an MPB arises when there is a *discontinuous* change in crystallline symmetry as a function of a *continuous* change in composition - in this case, the substitution of Zr for Ti. One signature of an MPB is a large change in atomic displacements as composition is changed. Hence for our case one might define an MPB as occurring when the ratio $r \equiv \frac{\delta\Delta x}{\delta n_{Zr}}$ is large. Here $\delta\Delta x$ is the change in atomic displacement (relative to the center of the O octahedra) on opposite sides of the possible MPB, and δn_{Zr} is the change in Zr content.

TABLE I. Calculated ferroelectric polarization (C/m^2) of PZT and the PZT-based alloys

Compound	P_x	P_y	P_z	P_{total}
PZT	0.070	0.066	0.805	0.811
PZT-BZnT	0.093	0.293	0.889	0.941
PZT-BZrT	0.416	0.579	0.080	0.718

We generate a dimensionless number for this ratio by considering the basic 5-atom unit cell (i.e. n_{Zr} varying between 0.375 and 0.5) and measuring the atomic displacements in units of the pseudo-cubic lattice parameter of this basic cell, which is 7.6905 a_B. Since the A-site cations drive the ferroelectricity in this system we focus our attention on the Pb and Bi displacements. From Figure 5, the Pb *c*-axis displacement changes by roughly 1.4 a_B, or approximately 0.18 of the cubic lattice parameter, for δn_{Zr} of 0.125, yielding a ratio *r* exceeding 1.4. This is a very large value - if this value were present over the entire 0 to 1 range of Zr content it would yield a change in displacement across the compositional range larger than the cubic lattice parameter, which is clearly impossible. The corresponding ratio *r* for the Bi *c*-axis displacement is 1.5. These values strongly suggest a large sensitivity of crystalline structure to relatively small changes in composition, reflective of an MPB.

B. Calculated ferroelectric polarization

In Table 1 we present the calculated ferroelectric polarization for the optimized PZT-BZnT and PZT-BZrT alloys (we also include PZT in its optimized tetragonal c/a=1.06 state for comparison). These polarizations were computed by calculating the Born effective charges of each of the atomic species in the unit cell using the program BerryPI[14] and multiplying these charges by the displacements of the atoms from their centrosymmetric values.

This approach was followed since any Berry-phase polarization computation program can only compute the ferroelectric polarization modulo[15] the polarization quantum $e\mathbf{R}/\Omega$, where *e* is the electric charge, $\mathbf{R}$ is a lattice vector and Ω the cell volume. For the large 2x2x2 supercells used this polarization quantum is approximately 25 μ C/cm^2, which is much smaller than the actual polarization. Hence the Born charge computation approach was used. We have checked that the polarization values from this method are close (within a few percent) to the values that would be obtained directly from BerryPI with an appropriate number of polarization quanta added.

We see immediately that the ferroelectric polarization of the PZT-BZnT alloy significantly exceeds that of PZT, with a total polarization of 0.94 C/m^2 in the PZT-BZnT alloy as opposed to 0.81 C/m^2 for PZT itself. The computed value for PZT is in good agreement with previously calculated values[12,16–20]. The value for PZT-BZrT is smaller, at 0.72 C/m^2, and largely arises from the planar displacements depicted in the bottom left of Fig. 5.

TABLE II. Calculated Born effective charges of atomic species in PZT and the PZT-BZnT alloy

PZT - tetrgonal			
Atomic Species	Z^*_{xx}	Z^*_{yy}	Z^*_{zz}
Pb	3.75	3.76	2.99
Zr	5.57	5.57	5.39
Ti	5.51	5.51	5.32
O	-3.15	-3.15	-2.84
PZT-BZnT			
Atomic Species	Z^*_{xx}	Z^*_{yy}	Z^*_{zz}
Pb	3.63	3.65	3.10
Bi	5.09	4.49	3.73
Zr	6.06	5.57	5.15
Ti	5.06	5.25	5.06
Zn	2.46	2.40	2.48
O	-3.03	-2.96	-2.68
PZT-BZrT			
Atomic Species	Z^*_{xx}	Z^*_{yy}	Z^*_{zz}
Pb	3.33	3.09	3.73
Bi	4.37	2.97	5.02
Zr	5.24	4.98	5.21
Ti	5.59	5.66	5.97
Zn	2.40	2.90	2.66
O	-2.87	-2.70	-3.08

It is of interest to examine the source of this increased ferroelectric polarization in PZT-BZnT more closely. In Table II we present the calculated BECs for each atomic species in PZT and PZT-BZnT, as well as PZT-BZrT. For Pb, the BECs are quite consistent in the two materials, varying by no more than a few percent. For the B-site cations Zr and Ti, five of the six BECs are in fact equal or *smaller* in PZT-BZnT than in PZT, and the oxygen charges are of slightly smaller magnitude in the PZT-BZnT alloy. The Bi BECs in PZT-BZnT are significantly larger than those of Pb, in keeping with the greater nominal ionic valence (+3 for Bi vs. +2 for Pb), while the BEC of Zn in PZT-BZnT is significantly smaller than that of its corresponding B-site cations Zr and Ti in PZT. All in all, it is clear there is no significant increase in the BECs upon alloying with BZnT.

The significant increase in calculated ferroelectric polarization for PZT-BZnT must therefore be attributed to the increased atomic displacements in the PZT-BZnT alloy. Specifically, the *c*-axis displacements of Pb in PZT from Figure 4 (top) of 1.1 Bohr are significantly outstripped by the 1.3 and 1.35 Bohr c-axis displacements of Pb and Bi in PZT-BZnT, respectively, in Figure 5 (top left). Both Pb and Bi also have significant planar displacements in the latter material, which contributes to the larger total polarization. Finally, the larger BEC of Bi makes an additional contribution (although this is partially cancelled by the smaller BEC of Zn in PZT-BZnT relative to Zr and Ti in PZT).

These results suggest that it is the smaller ionic radius of Bi, relative to Pb, that results in larger off-centerings and enhances the displacements of *both* atoms in the PZT-BZnT material, relative to the Pb displacements in PZT. This ultimately accounts for the improved ferroelectric properties of

PZT-BZnT relative to PZT.

It is of interest to briefly compare the BECs of PZT-BZrT with those of PZT-BZnT. One sees that the magnitude of these charges varies between these two compounds in no obvious manner: for example, the planar Zr Born effective charges are larger in PZT-BZnT while the opposite is true for the Ti effective charges. There is one consistent pattern, however: excepting Zn, in the tetragonal PZT-BZnT the c-axis BECs are smaller while in the quasi-monoclinic PZT-BZrT it is the planar BECs that are smaller. It is plausible that larger displacements correlate with smaller BECs.

To summarize these theoretical results, we find that within the pseudo-ternary PZT-BZnT system the addition of small amounts of BZnT increases both the ferroelectric polarization and the amount of tetragonality in the vicinity of the MPB. Thus it is of interest to determine whether material in this composition range can be readily synthesized by methods consistent with low cost production of the ceramic.

In the next section we discuss the elastic stability of the determined structures, followed by our experimental synthesis results on PZT-BZnT and PZT-BZnZr.

V. CONSIDERATION OF ELASTIC STABILITY

In this section we consider the elastic stability of the determined ground state structures. Since we have only conducted a structural search by varying c/a and optimizing internal coordinates, it is of interest to consider more general structural distortions. This is sometimes done by calculating phonon band structures across the entire Brillouin zone. Here we adopt a less computationally intensive approach and consider only elastic distortions.

For tetragonal structures, there are typically six or seven independent elastic constants[21], depending upon which symmetry class the crystal obeys; a similar statement applies to rhombohedral structures. In contrast, for a fully triclinic cell there are 21 independent elastic constants, and the elastic stability conditions for such a case are highly complex. Strictly speaking our relaxed structures are triclinic, as the structures were relaxed with *no* symmetry constraints. For the sake of practicality, we consider our cells to be tetragonal and consider the appropriate elastic constants $c_{11}, c_{12}, c_{13}, c_{33}, c_{44}$, and c_{66}. Note that c_{11} and c_{33} describe uniform elongation in the a and c directions, respectively, while c_{12} and c_{13} describe orthorhombic shearing motion in the ab and ac planes, respectively. c_{44} and c_{66} describe monoclinic shearing in the bc and ab planes, respectively.

In practical terms one evaluates these elastic constants by performing several strains, relaxing all internal coordinates, and then fitting the total computed energy as a function of the value of the strain. For example, uniform expansion of the a axis by a strain ε yields, in theory, an energy contribution $\frac{1}{2}c_{11}\varepsilon^2$. A good description of this procedure is found in Ref. 22. The most important consideration is that as many strains as possible be *isochoric*, or volume conserving, since one must carefully isolate the *volume* dependence of the total energy (particularly important for ferroelectrics) from the *strain* dependence.

For ferroelectric systems the calculation of elastic constants is complicated by the presence of a ferroelectric transition, or the existence of a finite *strain* despite zero applied *stress*. This means that the energy-strain curves may not necessarily obey a quadratic relation, complicating the analysis (see Figure 6). Rather than concern ourselves unnecessarily with this difficulty, we shall simply compute the total energy for several distinct strains and compare these with the ground state value.

The first of these is a uniform longitudinal strain (along all three axes) which results in a quadratic energy contribution $(c_{11}+c_{33}/2+c_{12}+2c_{13})\varepsilon^2$. Such a strain is often used to evaluate the bulk modulus, although it should be noted that the coefficient of ε^2 here is proportional to the *Voigt* bulk modulus, applicable to a polycrystalline sample, as opposed to that for a single crystal. In any case, the results of the strain are depicted in the insets of Fig. 6, for PZT-BZnT (top) and PZT-BZnZr (bottom) respectively. We see immediately that for both cases the energy curve is concave *upwards*, indicating the stability of these crystals under this strain. We note that, as is common with the LDA, the equilibrium volume is somewhat smaller than the experimental value - we find a uniform strain of approximately -0.010 (PZT-BZnZr) -0.013 (PZT-BZnT), or a volume 3-4 percent smaller than the experiment, to minimize the calculated energy. This is consistent with typical LDA volume errors.

The second strain we consider (termed "orthorhombic xy") is an expansion along a and compression along b, yielding a quadratic energy contribution $(c_{11}-c_{12})\varepsilon^2$. We see from the figures that both the PZT-BZnT and PZT-BZnZr are stable under this strain, although for the former the dependence is decidedly non-quadratic, and could exhibit a tiny instability around a strain of 0.005. Note that for all these volume conserving strains the energy is an even function of ε so we have simply symmetrized the curves. Similar behavior applies to the "orthorhombic xz" strain (quadratic energy contribution $c_{11}/2+c_{33}/2-c_{13}\varepsilon^2$), although in this case the PZT-BZnT energy is much more quadratic. It is interesting that for this more nearly tetragonal structure this energy is much smaller than in the PZT-BZnZr structure, which is more nearly monoclinic and on the "rhombohedral" side of the phase diagram. It is likely that the c-axis elongation ($c/a = 1.08$) of the PZT-BZnT structure reduces the elastic constants in the c direction.

Finally we consider the two shearing monoclinic strains "yz" and "xy", which yield contributions to the total energy proportional to c_{44} and c_{66}, respectively. Physically these correspond to a change in angle of the respective axis from 90^o and a tiny change in these lattice constants (to retain volume-conservation). For the "xy" monoclinic strain, the PZT-BZnT alloys is stable and well-behaved, with a tiny instability (~ 1 mev/u.c.) possible for PZT-BZnZr.

The situation is more complex for the "yz" monoclinic strain. The PZT-BZnZr alloy is stable under this strain, but the PZT-BZnT alloy shows an instability to this strain around $\varepsilon = 0.01$, with the minimum in energy approximately 25 meV per unit cell beneath the energy of the base optimized structure. This is rather unexpected. It may arise from some effective non-equivalence of the x and y axes. For example, for this

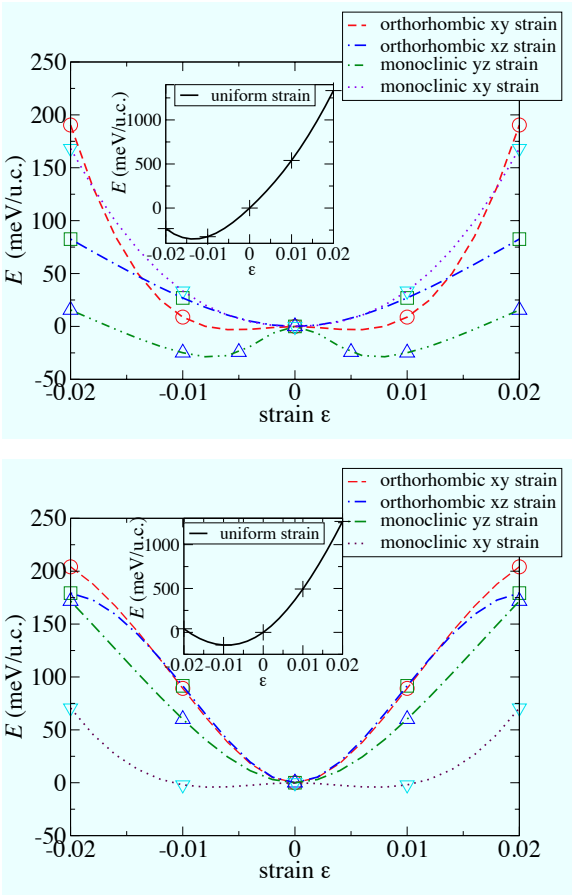

FIG. 6. (color online) The calculated energies (symbols) for distortions of the optimized PZT-BZnT (top) and PZT-BZnZr (bottom). The lines are spline fits of the calculated energies. See the text for explanations of the strains employed.

alloy in the large unit cell there are 4 Zr atoms but only 3 Ti atoms so that the rock-salt ordering of these atoms is necessarily disrupted; in a real alloy this non-equivalence would not likely occur. We note also that an instability of size less than 3 meV per formula unit (abbreviated f.u.), or 0.2 mRyd/f.u., is not a large one. For example, Ghita *et al*[23] calculate the optimized energy of PZT as 12.9 mRyd/f.u. lower than that of the symmetric perovskite structure; on this scale 0.2 mRyd is rather small. Finally, we have checked the displacement patterns of this structure (not shown), and find even larger cation displacements than in the PZT-BZnT structure reported earlier. Hence this structure, if it were present, would likely only *enhance* the ferroelectric properties of the PZT-BZnT alloy described above.

We note that we have not *proven* the stability of our optimized structures. This would require calculation of phonon dispersions, as well as consideration of the elastic stability conditions, as outlined in Ref. 21, and for the reasons presented previously actual calculation of the elastic constants is hampered by the ferroelectric nature of the systems studied here. Nevertheless, the fact that we find only one rather marginal instability for these two structures, as well as the experimental finding (below) of the stability of the alloys, suggest that the structures studied here are indeed stable.

In the next section we discuss the experimental work on sample synthesis and ferroelectric polarization measurements.

VI. EXPERIMENTAL SYNTHESIS AND STRUCTURAL DETERMINATION, POLARIZATION MEASUREMENTS AND COMPARISON TO THEORETICAL RESULTS

Polycrystalline samples of $(PZT)_{0.9}(BiZnT)_{0.1}$ and $(PZT)_{0.9}(BiZnZr)_{0.1}$ were prepared by standard ceramic techniques. Powders were mixed under 200 proof ethanol in an agate mortar and pestle, and firings were performed in air inside covered alumina crucibles with loose powders or pelletized samples. First $PbTiO_3$ and $PbZrO_3$ were made by reacting mixtures of PbO and TiO_2 or ZrO_2 at 850C for 12 h. These were mixed in equimolar proportions, pelletized and fired several times at 850 - 1000 C to form a precursor, multiphase material with composition $PbZr_{0.5}Ti_{0.5}O_3$. This was combined with Bi_2O_3, ZnO, and TiO_2 or ZrO_2, pelletized, and fired at 900 -1000C multiple times with intermediate grinding and pelletizing until single phase samples were formed.

A. Structural determination

Powder x-ray diffraction was performed using a PANalytical X'Pert Pro MPD with monochromatic Cu-Kα1 radiation to monitor phase purity of the samples and to determine crystallographic properties of the phases. The single phase $(PZT)_{0.9}(BiZnT)_{0.1}$ was found to be tetragonal with a = 4.0254(2) , c = 4.1389(2) and c/a = 1.028.The single phase $(PZT)_{0.9}(BiZnZr)_{0.1}$ was also found to be tetragonal with a = 4.0247(2) , c = 4.1360(2) and c/a = 1.028. We depict the tetragonal diffraction pattern from the latter compound in Fig.

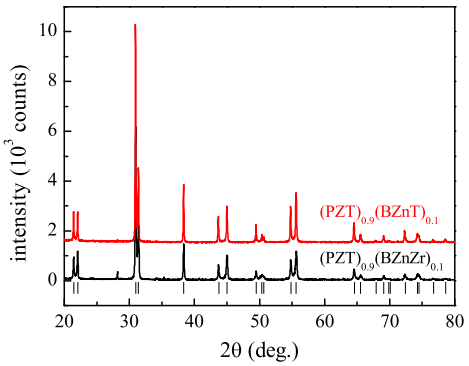

FIG. 7. (color online) The measured diffraction patterns from $(PZT)_{0.9}(BZnT)_{0.1}$ and $(PZT)_{0.9}(BZnZr)_{0.1}$. Tick marks locate the Bragg reflections for the tetragonal structure. All data are offset vertically for clarity.

7 below. Both c/a ratios are significantly larger than the av-

erage c/a value of 1.022 of PZT compositions near the MPB from the Inorganic Crystal Structure Database[13]. This is consistent with our theoretical finding of c/a ratios in the PZT-BZnT material larger than in PZT; in fact, the rate of increase in c/a ratio (0.006 for 10 percent BZnT substitution) is generally consistent with the theoretical c/a ratio increase of 0.02 (from 1.06 to 1.08) from PZT to $(PZT)_{0.75}$-$(BZnT)_{0.25}$ in our calculations.

We note that the experimental literature c/a ratio for PZT of 1.022 is significantly smaller than our calculated 1.06 value, so it is not surprising that our experimental c/a ratio of 1.028 for $(PZT)_{0.9}(BZnT)_{0.1}$ is smaller than the 1.08 value calculated for $(PZT)_{0.75}(BZnT)_{0.25}$, the BZnT proportion difference notwithstanding. Nevertheless, the experiment confirms the theoretically observed increased tetragonality associated with the alloying of BZnT with PZT, and is suggestive of increased ferroelectric polarization.

We note that our experiments find a tetragonal ground state for single-phase $(PZT)_{0.9}(BZnZr)_{0.1}$ whereas we have argued theoretically for the existence of an MPB based on the finding of a quasi-monoclinic phase in the calculations of the $(PZT)_{0.75}$-$(BZnZr)_{0.25}$ alloy.

One possible explanation for this discrepancy is that at the 10 percent BZnZr concentration, two competing ground states - tetragonal and rhombohedral, let us say - are sufficiently close in energy as to be switchable from extrinsic effects relating to sample preparation. We recall that the energy difference at the 25 percent BZnZr concentration studied theoretically is only 30 meV per unit cell, or 0.75 meV per atom, and assuming linearity would only be 0.3 meV per atom at a 10 percent BZnZr concentration. This may be sufficiently small that the details of the preparation conditions may in effect "switch" the material to a tetragonal state from its presumed monoclinic or rhombohedral ground state. Supporting this notion is the observation that during the initial synthesis efforts, the PZT-BZnZr sample contained a mixture of rhombohedral and tetragonal phases and that a single tetragonal phase was only achieved after multiple firings at 1000 C, suggesting the nearness of the two structures on the phase diagram.

B. Ferroelectric polarization measurements

Macroscopic ferroelectric polarization measurements were carried out with an aixACCT TF Analyzer 2000 at room temperature and a frequency of 100 Hz. For this purpose top and bottom silver electrodes were put down on the plate-like samples in order to measure in a parallel plate capacitor geometry. A high-voltage amplifier was used for the application of a maximum voltage of 200V. This is equivalent to an electric field of about 9.5 kV/cm and 7.7 kV/cm for the M1-214A and M1-235A samples, respectively. In both cases we do not find evidence of global ferroelectric switching. However, we find that the P(E) hysteresis loops open slightly, suggestive of ferroelectric polarization. We have ruled out the possibility of leakage currents causing the polarization by means of frequency dependent studies. This means that it is likely that ferroelectric behavior exists, but the electric fields tested were not large enough to overcome the potential barrier and induce polarization reversal. We cannot rule out the possibility that the samples are in fact paraelectric and that the observed small polarization is induced by the electric field. A linear approximation of the polarization response allowed us to estimate the dielectric constants ε_r of the sample materials; we find values of 598 and 764 for M1-214A and M1-235A, respectively. This indicates that M1-235A is either more ferroelectric or that it is closer to a ferroelectric transition.

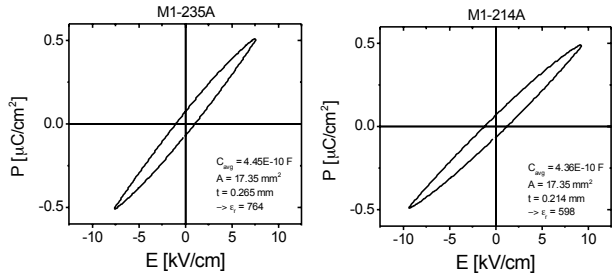

FIG. 8. (color online) The measured ferroelectric polarization of two PZT-based samples. Left, sample PZT-BZnZr; right sample PZT-BZnT.

It is somewhat surprising that the employed electric fields of order 10 kV/cm are not sufficient to induce significant ferroelectric polarization in the substituted alloys. While it is well known that thinner samples typically require correspondingly larger coercive fields, this is most an issue for samples of 1 micron or smaller thicknesses, not a few tenths of a millimeter as used here. However, one study on PZT[24] estimated a bulk coercive field for this material of 140 kV/cm. Another study[25] of PZT found a ferroelectric polarization of just 3 μC/cm^2 at a field of 30 kV/cm, indicative of a coercive field of order 1000 kV/cm. If the actual coercive field of the PZT-based alloys synthesized here is in the 140-1000 kV/cm range one would not expect much ferroelectric polarization at applied fields of 10 kV/cm. We think this is the likely origin of the small polarization measured here.

VII. CONCLUSION

Theoretical calculations on ordered supercells of PZT alloyed with $BiZn_{0.5}Ti_{0.5}O_3$ and $BiZn_{0.5}Zr_{0.5}O_3$ indicate significantly increased tetragonality (a c/a increase to 1.08 from 1.06) and ferroelectric polarization (0.94 C/m^2 vs. 0.81) relative to PZT, associated with the PZT-BZnT alloy. Altered displacement patterns between the two modeled alloy structures are suggestive of a morphotrophic phase boundary occurring at an intermediate composition. Experimental synthesis efforts demonstrate the feasibility of the proposed alloys and are consistent with the increased tetragonality predicted by theory. The experiment shows that in spite of the increased misfit of the ions with alloying the ceramic can be readily made. It will be of interest to explore higher Zr content mixtures to de-

termine the position of the MPB as well as to experimentally measure piezoelectric properties near that composition.

Acknowledgement. This work was supported by the U.S. Department of Energy (DOE), Office of Energy Efficiency and Renewable Energy, Vehicle Technologies, Propulsion Materials program (DP), and the DOE Office of Science, Basic Energy Sciences, Materials Sciences and Engineering Division (A.H., T.Z.W.).

[1] T.R. Shrout and S. J. Zhang. "Lead-free piezoelectric ceramics: Alternatives for PZT?" J. of Electroceramics **19**, 113 (2007).

[2] S. Park and T. R. Shrout. "Ultrahigh strain and piezoelectric behavior in relaxor based ferroelectric single crystals." J. Appl. Phys. **82**, 4 (1997).

[3] B. Jaffe. *Piezoelectric ceramics*. Vol. 3. Elsevier, 2012.

[4] T. Takenaka, K.-I. Maruyama, and K. Sakata. "$(Bi_{1/2}Na_{1/2})TiO_3$-$BaTiO_3$ system for lead-free piezoelectric ceramics." Japanese J. of Appl. Phys. **30.9S**, 2236 (1991).

[5] M. Ghita, M. Fornari, D. J. Singh, and S. V. Halilov. "Interplay between A-site and B-site driven instabilities in perovskites." Phys. Rev. B **72**, 054114 (2005).

[6] R.D.T. Shannon. "Revised effective ionic radii and systematic studies of interatomic distances in halides and chalcogenides." Acta Cryst. A **32**, 751 (1976).

[7] D.J. Singh and C. H. Park. "Polar behavior in a magnetic perovskite from A-site size disorder: a density functional study." Phys. Rev. Lett. **100**, 087601 (2008).

[8] I. Grinberg, M.R. Suchomel, W. Dmowski, S.E. Mason, H. Wu, P.K. Davies and A.M. Rappe, "Structure and polarization in the high T_c ferroelectric Bi (Zn, Ti) O_3-$PbTiO_3$ solid solutions". Phys. Rev. Lett. **98**, 107601 (2007).

[9] P.M. Gehring, S-E. Park, and G. Shirane. "Soft phonon anomalies in the relaxor ferroelectric Pb $(Zn_{1/3}Nb_{2/3})_{0.92}Ti_{0.08}O_3$." Phys. Rev. Lett. **84**, 5216 (2000).

[10] P. Blaha, K, Schwarz, G. Madsen, D, Kvasnicka and J. Luitz, WIEN2k, An Augmented Plane Wave + Local Orbitals Program for Calculating Crystal Properties (K. Schwarz, Tech. Univ. Wien, Austria, 2001).

[11] M. Suewattana, D. J. Singh, and S. Limpijumnong. "Crystal structure and cation off-centering in Bi $(Mg_{1/2}Ti_{1/2})$ O_3." Phys. Rev. B **86**, 064105 (2012). 064105.

[12] G. Saghi-Szabo, R. E. Cohen, and H. Krakauer. "First-principles study of piezoelectricity in tetragonal $PbTiO_3$ and $PbZr_{1/2}Ti_{1/2}O_3$." Phys. Rev. B **59**, 12771 (1999).

[13] PZT c/a ratios available from electronic search at https://icsd.fiz-karlsruhe.de.

[14] S.J. Ahmed, J. Kivinen, B. Zaporzan, Laura Curiel, Samuel Pichardo, and O. Rubel. "BerryPI: A software for studying polarization of crystalline solids with WIEN2k density functional all-electron package." Computer Physics Communications **184**, 647 (2013).

[15] K.M. Rabe et al. *Modern physics of ferroelectrics: essential background.* Springer:Berlin, Heidelberg, 2007.

[16] L. Bellaiche, and D. Vanderbilt. "Intrinsic piezoelectric response in perovskite alloys: PMN-PT versus PZT." Phys. Rev. Lett. **83**, 1347 (1999).

[17] L. Bellaiche, A. Garca, and D. Vanderbilt. "Finite-temperature properties of Pb $(Zr_{1-x}Ti_x)O_3$ alloys from first principles." Phys. Rev. Lett. **84**, 5427 (2000).

[18] C. Bungaro, and K. M. Rabe. "Lattice instabilities of $PbZrO_3$/$PbTiO_3$ [1: 1] superlattices from first principles." Phys. Rev. B **65**, 224106 (2002).

[19] I. Grinberg, V. R. Cooper, and A. M. Rappe. "Oxide chemistry and local structure of $PbZr_xTi_{1-x}O_3$ studied by density-functional theory supercell calculations." Phys. Rev. B **69**, 144118 (2004).

[20] R.E. Cohen. "Theory of ferroelectrics: a vision for the next decade and beyond." J. Phys. Chem. Solids **61**, 139 (2000).

[21] F. Mouhat and F.-X. Coudert. "Necessary and sufficient elastic stability conditions in various crystal systems." Phys. Rev. B **90**, 224104 (2014).

[22] G. Steinle-Neumann, L. Stixrude, and R. E. Cohen. "First-principles elastic constants for the hcp transition metals Fe, Co, and Re at high pressure." Phys. Rev. B **60**, 791 (1999).

[23] M. Ghita, M. Fornari, D. J. Singh, and S. V. Halilov. "Interplay between A-site and B-site driven instabilities in perovskites." Phys. Rev. B **72**, 054114 (2005).

[24] N.A. Pertsev, J. Rodriguez Contreras, V. G. Kukhar, B. Hermanns, H. Kohlstedt, and R. Waser. "Coercive field of ultrathin Pb $(Zr_{0.52}Ti_{0.48})$ O_3 epitaxial films." Appl. Phys. Lett. **83**, 3356 (2003).

[25] D.V. Taylor, and D. Damjanovic. "Evidence of domain wall contribution to the dielectric permittivity in PZT thin films at sub-switching fields." J. Appl. Phys. **82**, 1973 (1997).